Measurement of cosmic-ray energy spectrum with the TALE detector in hybrid mode

H. Oshima,[a,*] **K. Fujita,**[a] **S. Ogio**[a] **and T. Sako**[a] **for the Telescope Array Collaboration**

[a]*Institute for Cosmic Ray Research, the University of Tokyo,*
5-1-5 Kashiwa-no-ha, Kashiwa, Chiba, Japan

E-mail: oshima@icrr.u-tokyo.ac.jp

The TA Low-energy Extension (TALE) experiment extends the low-energy side of the TA experiment below 10^{15} eV. A main objective of TALE is to study the transition from galactic to extragalactic cosmic rays. The TALE detector is a hybrid observatory composed of fluorescence telescopes and a surface detector array of scintillation counters. The surface detectors are arranged with inter-counter spacing of 400 and 600 meters, suitable for hybrid energy spectrum measurements in the low-energy region. We measured the energy spectrum using data collected during 429 hours of observation by the TALE hybrid detector. This energy spectrum measurement will play an important role in understanding the transition from cosmic rays of galactic origin to those of extragalactic origin.

ICRC2023
38th International Cosmic Ray Conference
The Astroparticle Physics Conference

---

*Speaker

1. Introduction

More than 100 years have passed since the discovery of cosmic rays, but the origin of ultra-high energy cosmic rays (UHECRs) has not been revealed yet. Revealing the UHECR origins is one of the most important topics of cosmic-ray physics. Galactic cosmic rays originate within the Milky Way Galaxy, while extragalactic cosmic rays originate outside the galaxy. In the energy region below $10^{18.7}$ eV, galactic and extragalactic cosmic rays are in competition with each other. Shape of the energy spectrum reflects various physical phenomena such as the transition from galactic to extragalctic cosmic rays, the characteristics and acceleration limits of galactic cosmic ray, and confinement by the galactic magnetic field. In order to unravel the intricately intertwined information, it is essential to measure the cosmic-ray energy spectrum and the composition over a wide energy range. We cover the wide energy range of five orders of magnitude from 10^{15} eV to 10^{20} eV by both the Telescope Array (TA) [1, 2] and the TA Low-energy Extension (TALE) [3, 4] experiments. We aim to measure the acceleration limit of galactic cosmic rays through the measurements of composition and energy spectrum, and the transition from galactic to extragalactic cosmic rays using the TALE detector.

2. TALE detector and data samples

TA is the largest cosmic-ray detector in the Northern Hemisphere, located in Millard County, Utah, USA. The TALE experiment extends the energy range observed by the TA experiment to lower energies. The TALE detector is suitable to study the energy spectrum structure and the associated change in the composition of cosmic rays below $10^{18.6}$ eV. The TALE detector is a hybrid apparatus composed of scintillation surface detectors (SDs) covering an area of approximately $20\,\mathrm{km^2}$ and fluorescence telescopes (FDs) overlooking the SDs, as shown in Fig. 1. The TALE SDs are placed at $400\,\mathrm{m}$ and $600\,\mathrm{m}$ spacing for low-energy thresholds. In this study, we analyzed data sample between November 2018 and February 2020 corresponding to 429 hours of operation. These data are collected using both the FDs and the SDs.

3. Monte Carlo simulation

Detector aperture is evaluated using a Monte Carlo (MC) simulation. The MC simulations used in this work include the generation of extensive air showers by cosmic ray primaries and the detector response to these showers. Air-shower simulations are generated with the CORSIKA program [5] using QGSJet II-04 [6] hadronic interaction model at high energies. Proton- and iron-induced air showers are generated with primary energies ranging from $10^{16.2}$ eV to $10^{18.5}$ eV. The proton and iron primaries are mixed using the fraction based on the H4a composition model [7]. These showers are thrown with an isotropic zenith angle distribution between 0° and 70° and a uniform azimuthal distribution between 0° and 360°. Particle information such as position and momentum at the detector level is used to obtain the energy deposit in each SD with the GEANT code [8–10]. The response of the SD electronics is also taken into account [11]. The FD simulation includes fluorescence and Cherenkov photon generations, telescope optics [12], detector calibration [13], and the response of the electronics [14, 15].

2
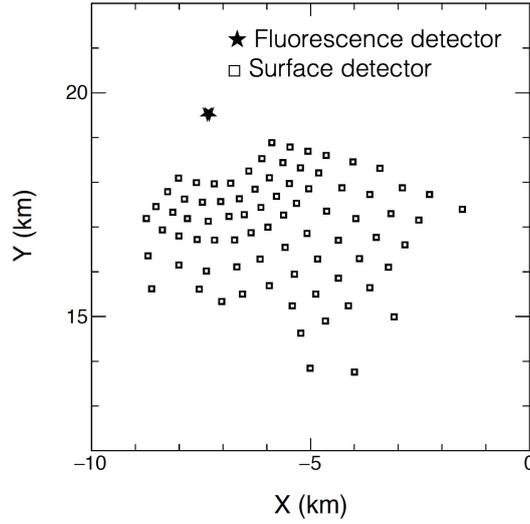
Figure 1: Physical location of TALE detector. The TALE detector is a hybrid apparatus composed of surface detectors and fluorescence detectors.

4. Data analysis

The analysis is based on hybrid data collected by the TALE FDs and SDs. One of the advantages of hybrid observation is that the depth of maximum, X_{max}, of the air shower which is a sensitive quantity for composition analysis is measured by FDs. In addition, the SD array is used to determine the shower axis and it improves the energy resolution compared to the FD mono observation. We used events which are triggered by the FDs and have at least one SD with a signal above one minimum ionizing particle energy loss. In this analysis, we used only the top 10 telescopes that observe fields of view at high elevation angles.

Image of the air shower observed by FDs is referred to as the event track. The following conditions are required to select event tracks that have high quality reconstruction: 1) there is no saturated PMT in the track; 2) X_{max} of the air shower is within the field of view of the FDs; and 3) the reduced χ^2 in the fitting of longitudinal development of the air shower is less than 100.

As the air shower develops, both the atmospheric fluorescence and the Cherenkov light are emitted. Cherenkov light is the dominant component below $10^{17.0}$ eV, while the fluorescence component increases with increasing energy, becoming the main component above $10^{17.5}$ eV. Events with the fraction of fluorescence light above 75% are defined as fluorescence events, while the others are defined as Cherenkov events. Several filtering criteria are then applied to select shower-induced track-like events. Regarding the Cherenkov events, the following conditions are required: 1) event duration is above 0.1 μs; 2) the number of PMTs constituting the track is at least 10; 3) the average number of photo-electrons/PMT is greater than 50; and 4) the track length is greater than 6.5°. Concerning the fluorescence events, the sum of the number of photo-electrons in all PMT's is required to be at least 2000 per event. In addition to these filtering conditions, the zenith angle acceptance was set to $\theta < 60°$, while the energy range was set between $10^{16.5}$ eV and $10^{18.1}$ eV.

The measured energy spectrum is not an exact representation of the true energy spectrum due to the detector efficiency and resolution. Therefore, an unfolding is performed to correct the

smearing between the true spectrum and the measured spectrum. In this analysis, we used the Iterative unfolding method proposed by D'Agostini [16, 17]. This unfolding method is based on Bayes' theorem and the unsmearing can be written as

$$C'_i = \sum_{j=1}^{N_m} U_{ij} E_j^{data},$$ (1)

where C'_i is a number of true events in the i-th true energy bin, N_m is a number of bins of measured spectrum, U_{ij} is an unsmearing matrix, and E_j^{data} is a number of events in the j-th measured energy bin. Figure 2 shows a resolution map between true and measured energies. The resolution map is evaluated by the MC simulation. Unsmearing matrix can be calculated by the resolution map. Figure 3 shows true, measured, and unfolded spectra in the MC simulation. The unfolded spectrum is obtained through the unsmearing process of the measured spectrum based on the unsmearing matrix. Figure 3 shows that the unsmearing process is successfully performed and the unfolded spectrum is consistent with the true spectrum.
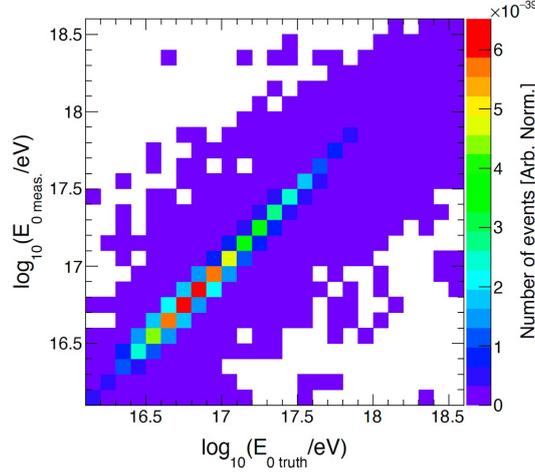
Figure 2: Resolution map between true and measured energies. The resolution map is evaluated by the MC simulation.

The product of the effective aperture and the observation time is called the effective exposure. Figure 4 shows the effective exposure used in this analysis. The effective exposure is evaluated by the MC simulation. Exposure in the high energy region above 10^{18} eV decreases because the ground array size is fixed and the TALE FDs observe a field of view with a high elevation angle, thus the number of events with a depth of shower maximum out of the field of view increases. Energy spectrum is expressed as

$$J(E_i) = \frac{\sum_{j=1}^{N_m} U_{ij} N_j^{sel}}{A\Omega(E_i) \cdot T \cdot \Delta E_i},$$ (2)

where $J(E_i)$ is the flux in the i-th energy bin, U_{ij} is the unsmearing matrix, N_j^{sel} is the number of selected events in the j-th measured energy bin, $A\Omega(E_i)$ is the effective aperture, T is the observation time, and ΔE_i is a width of the i-th bin.
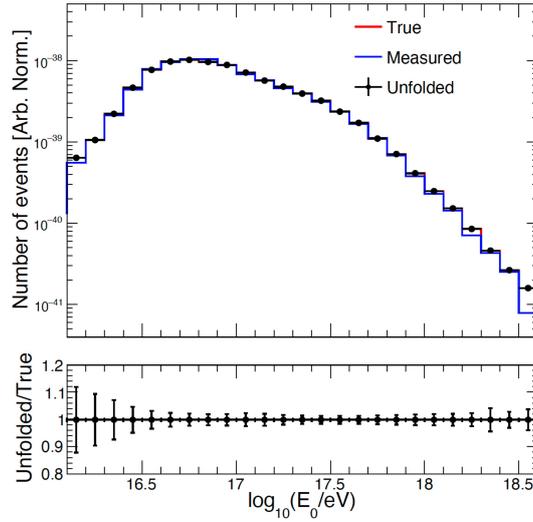
Figure 3: Top half of the figure shows true, measured, and unfolded energy spectra, while the bottom half shows the ratio of unfolded and true distributions. The unfolded spectrum is obtained through the unsmearing process of the measured spectrum based on the unsmearing matrix. The unsmearing is successfully performed and the unfolded spectrum is consistent with the true spectrum.
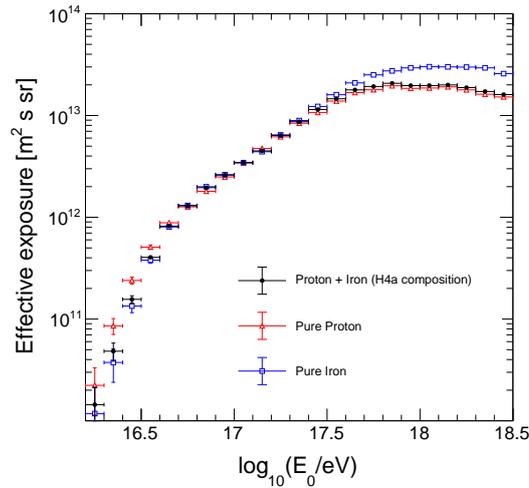

Figure 4: Effective exposure in this analysis. The effective exposure is expressed as a function of the true energy. This exposure is evaluated by the MC simulation.

5. Results

Figure 5 shows the distributions of the parameters related to reconstructed shower geometrical parameters which are core positions X and Y, zenith angle, azimuth angle, Ψ angle, and R_p. The Ψ angle is the angle of the shower axis with respect to the direction of the center of the shower track and R_p is the shower impact parameter to the detector.

Figure 6 shows the energy distribution of the events. The energy resolutions are 10.1% and 8.6% for proton- and iron-induced air showers, respectively, which are evaluated by the MC simulation
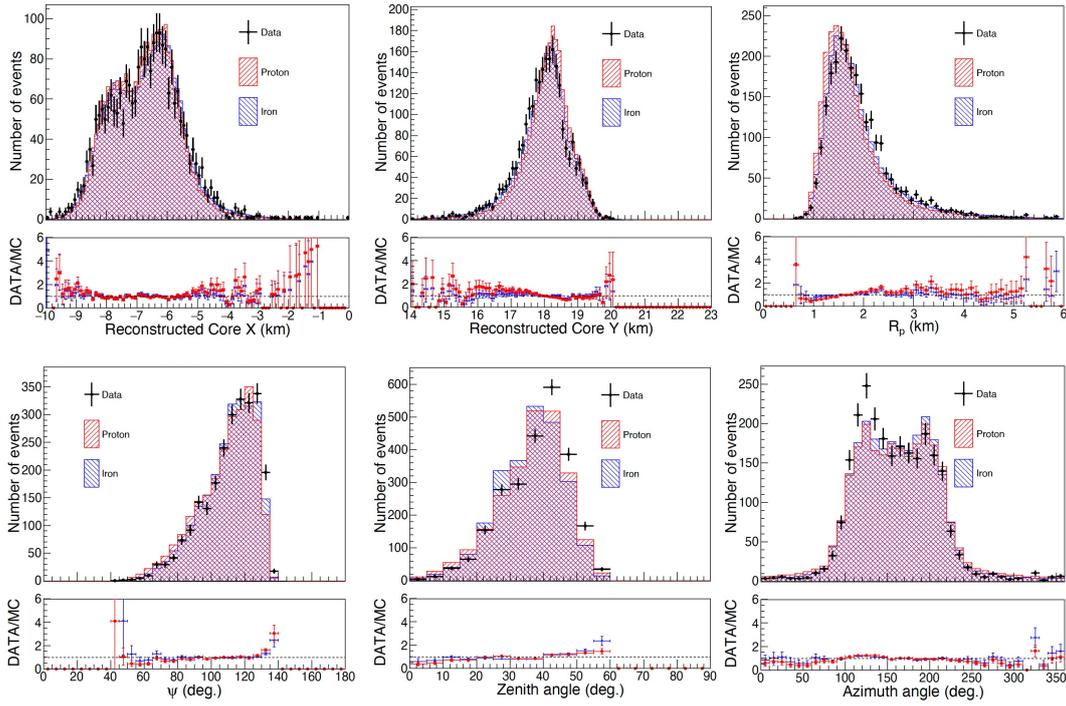
Figure 5: Distributions of reconstructed shower geometrical parameters. The data are shown by marker points, while the MC prediction are shown by red and blue histograms for pure proton and pure iron, respectively. The MC predictions are normalized to the number of events in the data.

and they are consistent with those from the previous study [18].

Figure 7 shows the result of energy spectrum obtained in this study, as well as that reported by TALE FD mono observation [3]. In this analysis, the TALE hybrid observation data was used. The analysis with more statistics is on-going and the expected statistics will increase to around four times. Note that the MC studies with other hadronic interaction model and compositions are also in progress.

6. Summary

It is important to measure the acceleration limit of galactic cosmic rays through the measurements of composition and energy spectrum and to understand the transition from galactic to extragalactic cosmic rays. To study those physical topics, it is essential to measure the cosmic-ray energy spectrum and the composition over a wide energy range. Combining the TA and TAx4 as well as TALE observation data, the energy spectrum is measured over five orders of magnitude from 10^{15} eV to 10^{20} eV. In this work, we observed and analyzed the cosmic-ray events using the TALE detector. We checked the fundamental information, such as core positions, and measured the energy spectrum with the TALE hybrid mode. In this talk, we presented the preliminary result with a part of the TALE hybrid observation corresponding to the 429 hours observation data. The analysis with more statistics is on-going and the expected statistics would increase to around four times. This energy spectrum measurement will play an important role in understanding the transition from cosmic rays of galactic origin to those of extragalactic origin.
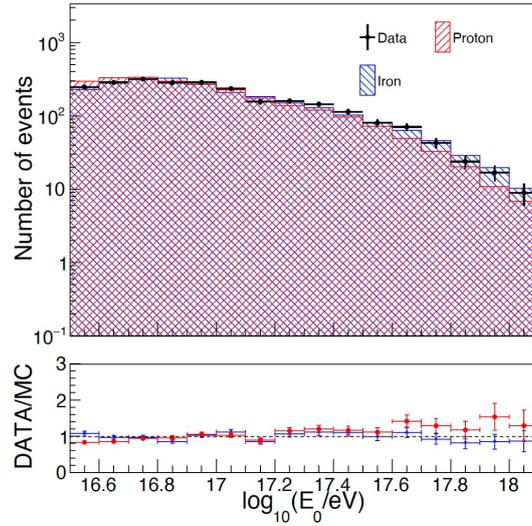
Figure 6: Comparisons of the measured energy distributions between the data and the MC predictions. The data are shown by marker points, while the MC prediction are shown by red and blue histograms for pure proton and pure iron, respectively. The MC predictions are normalized to the number of events in the data.
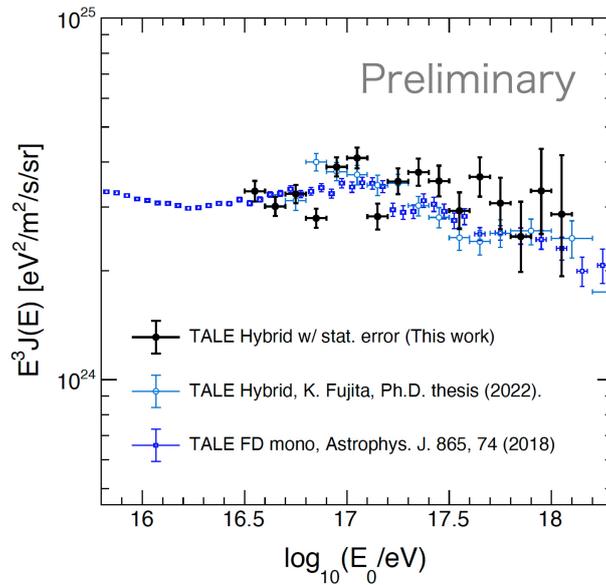

Figure 7: The result of energy spectrum. The spectrum obtained in this analysis is shown by black marker points, while that reported by TALE FD mono observation is shown by blue ones.

Acknowledgements

References

[1] H. Kawai *et al.* (TA Collaboration), J. Phys. Soc. Jpn. Suppl. A **78**, 108 (2009).

[2] T. Abu-Zayyad *et al.* (TA Collaboration), Astrophys. J. Lett. **768**, L1 (2013).

[3] R. U. Abbasi *et al.* (TA Collaboration), Astrophys. J. **865**, 74 (2018).

[4] R. U. Abbasi *et al.* (TA Collaboration), Astrophys. J. **909**, 178 (2021).

[5] D. Heck, G. Schatz, T. Thouw, J. Knapp, and J.N. Capdevielle, Tech. Rep. FZKA **6019** (1998).

[6] S. Ostapchenko, Nucl. Phys. B, Proc. Suppl. **151**, 143 (2006).

[7] T. K. Gaisser, Astropart. Phys. **35**, 801 (2012).

[8] S. Agostinelli *et al.*, Nucl. Instrum. Methods Phys. Res., Sect. A **506**, 250 (2003).

[9] J. Allison *et al.*, IEEE Trans. Nucl. Sci. **53**, 270 (2006).

[10] J. Allison *et al.*, Nucl. Instrum. Methods Phys. Res., Sect. A **835**, 186 (2016).

[11] T. Abu-Zayyad *et al.* (TA Collaboration), Nucl. Instrum. Methods Phys. Res. A **689**, 87 (2012).

[12] H. Tokuno *et al.* (TA Collaboration), Nucl. Instrum. Methods Phys. Res. A **676**, 54 (2012).

[13] H. Tokuno *et al.* (TA Collaboration), Nucl. Instrum. Methods Phys. Res. A **601**, 364 (2009).

[14] A. Taketa *et al.* (TA Collaboration), Proceedings of the 29th International Cosmic Ray Conference, Pune, India, vol. **8**, 209 (2005).

[15] Y. Tameda *et al.* (TA Collaboration), Nucl. Instrum. Methods Phys. Res. A **609**, 227 (2009).

[16] G. D'Agostini, Nucl. Instrum. Methods Phys. Res., Sect A **362**, 487 (1995).

[17] G. D'Agostini, arXiv:1010.0632

[18] K. Fujita, Ph.D. thesis, Osaka City University (2022).

Full Authors List: The Telescope Array Collaboration
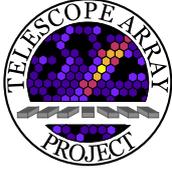
R.U. Abbasi[1], Y. Abe[2], T. Abu-Zayyad[1,3], M. Allen[3], Y. Arai[4], R. Arimura[4], E. Barcikowski[3], J.W. Belz[3], D.R. Bergman[3], S.A. Blake[3], I. Buckland[3], B.G. Cheon[5], M. Chikawa[6], A. Fedynitch[6,7], T. Fujii[4,8], K. Fujisue[6], K. Fujita[6], R. Fujiwara[4], M. Fukushima[6], G. Furlich[3], Z. Gerber[3], N. Globus[9*], W. Hanlon[3], N. Hayashida[10], H. He[9], R. Hibi[2], K. Hibino[10], R. Higuchi[9], K. Honda[11], D. Ikeda[10], N. Inoue[12], T. Ishii[11], H. Ito[9], D. Ivanov[3], A. Iwasaki[4], H.M. Jeong[13], S. Jeong[13], C.C.H. Jui[3], K. Kadota[14], F. Kakimoto[10], O. Kalashev[15], K. Kasahara[16], S. Kasami[17], S. Kawakami[4], K. Kawata[6], I. Kharuk[15], E. Kido[9], H.B. Kim[5], J.H. Kim[3], J.H. Kim[3†], S.W. Kim[13], Y. Kimura[4], I. Komae[4], K. Komori[17], Y. Kusumori[17], M. Kuznetsov[15,18], Y.J. Kwon[19], K.H. Lee[5], M.J. Lee[13], B. Lubsandorzhiev[15], J.P. Lundquist[3,20], T. Matsuyama[4], J.A. Matthews[3], J.N. Matthews[3], R. Mayta[4], K. Miyashita[2], K. Mizuno[2], M. Mori[17], M. Murakami[17], I. Myers[3], S. Nagataki[9], K. Nakai[4], T. Nakamura[21], E. Nishio[17], T. Nonaka[6], S. Ogio[6], H. Ohoka[6], N. Okazaki[6], Y. Oku[17], T. Okuda[22], Y. Omura[4], M. Onishi[6], M. Ono[9], A. Oshima[23], H. Oshima[6], S. Ozawa[24], I.H. Park[13], K.Y. Park[5], M. Potts[3‡], M.S. Pshirkov[15,25], J. Remington[3], D.C. Rodriguez[3], C. Rott[3,13], G.I. Rubtsov[15], D. Ryu[26], H. Sagawa[6], R. Saito[2], N. Sakaki[6], T. Sako[6], N. Sakurai[4], D. Sato[2], K. Sato[4], S. Sato[17], K. Sekino[6], P.D. Shah[3], N. Shibata[17], T. Shibata[6], J. Shikita[4], H. Shimodaira[6], B.K. Shin[26], H.S. Shin[6], D. Shinto[17], J.D. Smith[3], P. Sokolsky[3], B.T. Stokes[3], T.A. Stroman[3], Y. Takagi[17], K. Takahashi[6], M. Takamura[27], M. Takeda[6], R. Takeishi[6], A. Taketa[28], M. Takita[6], Y. Tameda[17], K. Tanaka[29], M. Tanaka[30], S.B. Thomas[3], G.B. Thomson[3], P. Tinyakov[15,18], I. Tkachev[15], H. Tokuno[31], T. Tomida[2], S. Troitsky[15], R. Tsuda[4], Y. Tsunesada[4,8], S. Udo[10], F. Urban[32], I.A. Vaiman[15], D. Warren[9], T. Wong[3], K. Yamazaki[23], K. Yashiro[27], F. Yoshida[17], Y. Zhezher[6,15], and Z. Zundel[3]

[1] *Department of Physics, Loyola University Chicago, Chicago, Illinois 60660, USA*
[2] *Academic Assembly School of Science and Technology Institute of Engineering, Shinshu University, Nagano, Nagano 380-8554, Japan*
[3] *High Energy Astrophysics Institute and Department of Physics and Astronomy, University of Utah, Salt Lake City, Utah 84112-0830, USA*
[4] *Graduate School of Science, Osaka Metropolitan University, Sugimoto, Sumiyoshi, Osaka 558-8585, Japan*
[5] *Department of Physics and The Research Institute of Natural Science, Hanyang University, Seongdong-gu, Seoul 426-791, Korea*
[6] *Institute for Cosmic Ray Research, University of Tokyo, Kashiwa, Chiba 277-8582, Japan*
[7] *Institute of Physics, Academia Sinica, Taipei City 115201, Taiwan*
[8] *Nambu Yoichiro Institute of Theoretical and Experimental Physics, Osaka Metropolitan University, Sugimoto, Sumiyoshi, Osaka 558-8585, Japan*
[9] *Astrophysical Big Bang Laboratory, RIKEN, Wako, Saitama 351-0198, Japan*
[10] *Faculty of Engineering, Kanagawa University, Yokohama, Kanagawa 221-8686, Japan*
[11] *Interdisciplinary Graduate School of Medicine and Engineering, University of Yamanashi, Kofu, Yamanashi 400-8511, Japan*
[12] *The Graduate School of Science and Engineering, Saitama University, Saitama, Saitama 338-8570, Japan*
[13] *Department of Physics, SungKyunKwan University, Jang-an-gu, Suwon 16419, Korea*
[14] *Department of Physics, Tokyo City University, Setagaya-ku, Tokyo 158-8557, Japan*
[15] *Institute for Nuclear Research of the Russian Academy of Sciences, Moscow 117312, Russia*
[16] *Faculty of Systems Engineering and Science, Shibaura Institute of Technology, Minato-ku, Tokyo 337-8570, Japan*
[17] *Graduate School of Engineering, Osaka Electro-Communication University, Neyagawa-shi, Osaka 572-8530, Japan*
[18] *Service de Physique Théorique, Université Libre de Bruxelles, Brussels, Belgium*
[19] *Department of Physics, Yonsei University, Seodaemun-gu, Seoul 120-749, Korea*
[20] *Center for Astrophysics and Cosmology, University of Nova Gorica, Nova Gorica 5297, Slovenia*
[21] *Faculty of Science, Kochi University, Kochi, Kochi 780-8520, Japan*
[22] *Department of Physical Sciences, Ritsumeikan University, Kusatsu, Shiga 525-8577, Japan*
[23] *College of Science and Engineering, Chubu University, Kasugai, Aichi 487-8501, Japan*
[24] *Quantum ICT Advanced Development Center, National Institute for Information and Communications Technology, Koganei, Tokyo 184-8795, Japan*
[25] *Sternberg Astronomical Institute, Moscow M.V. Lomonosov State University, Moscow 119991, Russia*
[26] *Department of Physics, School of Natural Sciences, Ulsan National Institute of Science and Technology, UNIST-gil, Ulsan 689-798, Korea*
[27] *Department of Physics, Tokyo University of Science, Noda, Chiba 162-8601, Japan*
[28] *Earthquake Research Institute, University of Tokyo, Bunkyo-ku, Tokyo 277-8582, Japan*
[29] *Graduate School of Information Sciences, Hiroshima City University, Hiroshima, Hiroshima 731-3194, Japan*
[30] *Institute of Particle and Nuclear Studies, KEK, Tsukuba, Ibaraki 305-0801, Japan*
[31] *Graduate School of Science and Engineering, Tokyo Institute of Technology, Meguro, Tokyo 152-8550, Japan*
[32] *CEICO, Institute of Physics, Czech Academy of Sciences, Prague 182 21, Czech Republic*

∗ Presently at: University of California - Santa Cruz
† Presently at: Argonne National Laboratory, Physics Division, Lemont, Illinois 60439,USA
‡ Presently at: Georgia Institute of Technology, Physics Department, Atlanta, Geogia 30332,USA